

## Appendix B

### Flow-Induced Crystallization of Model Systems

<b>B.1 INTRODUCTION.....</b>	<b>B-2</b>
<b>B.2 EXPERIMENTAL METHODS.....</b>	<b>B-4</b>
<b>B.2.1 Materials .....</b>	<b>B-4</b>
B.2.1.2 Overlap Concentration .....	B-5
<b>B.2.2 Shear-Induced Crystallization .....</b>	<b>B-6</b>
<b>B.3 RESULTS.....</b>	<b>B-6</b>
<b>B.4 DISCUSSION .....</b>	<b>B-7</b>
<b>B.5 CONCLUSION.....</b>	<b>B-10</b>
<b>B.6 ACKNOWLEDGEMENTS.....</b>	<b>B-10</b>
<b>B.7 REFERENCES.....</b>	<b>B-12</b>

## B.1 INTRODUCTION

The physical properties of semicrystalline materials are ultimately dictated by their morphology in the solid state, which is a strong function of the response of the polymer melt to processing conditions. Under certain conditions, the formation of oriented nuclei under flow produces an oriented morphology,<sup>1</sup> which results in increased crystallization kinetics and enhancement of physical properties.<sup>2-6</sup> The formation of oriented nuclei in part depends on the perturbation of crystallizable chains from their equilibrium configurations in the melt. The degree of chain orientation is dictated by their relaxation dynamics relative to an applied flow field.<sup>3</sup> Highly branched materials relax through a hierarchy of motions,<sup>7</sup> hence, materials with well-defined architectures, such as hydrogenated polybutadienes (HPBDs),<sup>8-12</sup> are ideal systems with which to probe the effects of melt dynamics on flow-induced crystallization (FIC) of semicrystalline polymers.<sup>13</sup>

The effect of the slow-relaxing species (i.e., the model HPBD) can be examined through the implementation of bimodal blends which contain a small concentration of the slow-relaxing species in a fast-relaxing matrix. These model bimodal systems are common in FIC studies, in which they are usually composed of two species with substantially different molecular weights (e.g., Chapter 5).<sup>14-19</sup> The concentration of the slow relaxing species has a non-linear effect on FIC behavior; greatly enhanced crystallization kinetics and development of oriented morphology are observed near its overlap concentration,  $c^*$ , at which chains just pervade all sample volume (Figure B.1).<sup>13-</sup>

<sup>15</sup> Hence, although it is important to keep the concentration of the slow-relaxing species

low in order to minimize its effects on the viscosity of the blend (and to not introduce a new experimental variable), the concentrations need to be at least as high as  $c^*$  to observe pronounced FIC effects.

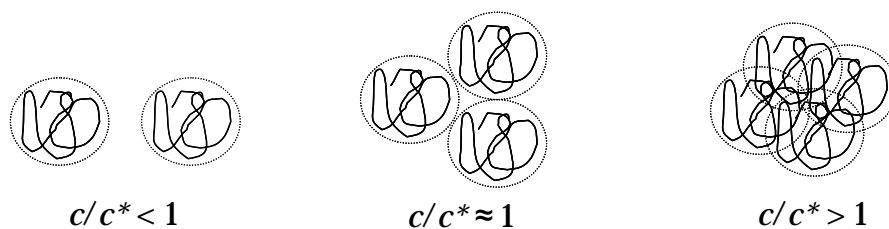


**Figure B.1** Schematic representation of overlap concentration,  $c^*$ .

The major component of the bimodal blend must meet particular requirements with regard to the study of HPBD materials. Due to the nature of anionic polymerization, which is used to synthesize model HPBDs, the resulting materials contain short-chain branches (SCB) and are analogous to random ethylene-co-butenes with a minimum of 4 mol % butene.<sup>20, 21</sup> In order to de-convolute the effects of relaxation dynamics from short-chain branching, it necessary to select a base resin containing comparable amounts of SCB.

In the following section, we present preliminary FIC studies on a bimodal blend containing an HPBD comb polymer in an ethylene-co-hexene matrix with comparable SCB content. This comb polymer, which exhibits two relaxation processes—that of the arms followed by that of the backbone<sup>22</sup>—was anticipated to have a profound effect on oriented morphology following shear.

## B.2 EXPERIMENTAL METHODS

### B.2.1 Materials

Molecular characteristics of the bimodal blend components are provided in Figure B.2 and Table B.1. The minor component in the bimodal blends was a hydrogenated polybutadiene (HPBD) comb polymer (C4) synthesized via anionic polymerization, followed by hydrogenation, in conjunction with hydrosilylation.<sup>8, 20</sup> This molecule contained an average of 4 teeth per backbone. The polydispersity ( $PDI = M_w/M_n$ ) of the comb backbone and teeth components was below 1.05, but since the number of teeth per backbone is an average, the combs themselves could not be considered monodisperse. Similar to the H4 polymer in Chapter 3, C4 exhibited intrachain heterogeneity in the SCB distribution due to the synthetic route to the telechelic backbone; the teeth contained approximately 19 SCB per 1000 backbone carbon atoms while the backbone contained higher SCB content (approximately 40 SCB/1000 backbone C). C4 was graciously provided by Professor Nikos Hadjichristidis (University of Athens, Athens, Greece) and characterized by Dr. David Lohse and his team (ExxonMobil, Clinton, NJ).

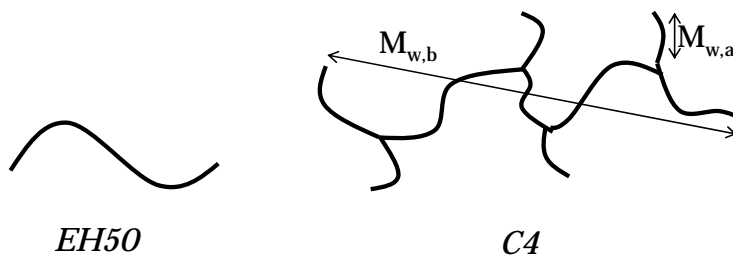


**Figure B.2** Schematic representation of bimodal blend components.

**Table B.1 Molecular characteristics of blend components studied under flow. All values provided by ExxonMobil.**

Polymer	Type	$M_{w,tot}$ (kg/mol)	PDI	$M_{w,b}$ (kg/mol)	$M_{w,a}$ (kg/mol)	SCB/ 1000 backbone $C^a$
EH50	linear	50	2.0	50		23.2
C4 <sup>b</sup>	comb	232		100	33	24.4

<sup>a</sup> obtained via <sup>13</sup>C NMR

The major component in the bimodal blends was metallocene-catalyzed random ethylene copolymer with approximately 5 mol % hexene. Given the strong dependence of crystallization behavior on SCB content, EH50 was selected due to its similar SCB content in an attempt to isolate the effects of LCB and SCB. EH50 was graciously provided and characterized by Dr. David Lohse and his team (ExxonMobil, Clinton, NJ).

Blends containing 1, 1.5 and 5 wt % C4 in EH50 were created as described in Chapter 5. Comb concentrations in the blends were selected to be above and below their overlap concentration,  $c^* \approx 0.012$ , which is the concentration at which chains just pervade all sample volume resulting in a non-linear response to the flow field.<sup>13-15</sup> An estimate of  $c^*$  was made based on the comb backbone length,  $M_{w,b}$ , as done by Heeley et al.<sup>13</sup>

### B.2.1.2 Overlap Concentration

If we assume that the backbone is the only part of the comb oriented by flow, it is possible to estimate the overlap concentration,  $c^*$ , for comb-comb contact as that of a linear chain having comparable molecular weight to the backbone ( $M_{w,b}$ ), as done by Heeley et al.<sup>13</sup> Hence,

$$c^* = \frac{3M_{w,b}}{4\pi(R_g^2)^{3/2} \rho N_a}, \quad (\text{B.1})$$

where  $N_a$  is Avogadro's number,  $\rho$  is density, and  $R_g$  is the radius of gyration.<sup>23,</sup>

<sup>24</sup> From small-angle neutron scattering measurements,  $R_g(\text{\AA})$  for linear hydrogenated polybutadienes was found to depend on  $M_{w,tot}$  (g/mol) as<sup>25</sup>

$$R_g = 0.5 (M_{w,tot})^{1/2}. \quad (\text{B.2})$$

Using eqs B.1 and B.2, we find that  $c^* \approx 0.012$ . As this is a rough approximation, blends of 1, 1.5 and 5 wt % comb in EH50 were made.

### B.2.2 Shear-Induced Crystallization

Isothermal crystallization of comb blends following a short shear pulse was studied using the same instrument and protocol as described in Section 5.2.3 of Chapter 5. The isothermal crystallization temperature used was  $T_c = 98$  °C. Wall shear stresses ( $\sigma_w$ ) imposed were 0.11 MPa for a shearing time ( $t_s$ ) of 10 s and 0.14 MPa for  $t_s = 15$  s. The total sample mass extruded, and hence the total strain, was kept relatively constant just below 100 mg. Morphology development was followed in situ via optical transmittance ( $I/I_0$ ) and apparent birefringence ( $I_{perp}/I$ ) measurements.

## B.3 RESULTS

Shear was found to have no effect on the crystallization of 1 or 1.5 wt % comb blends. Apparent birefringence revealed no orientation and crystallization kinetics (as given by transmittance) were unchanged from the quiescent case (not shown). The 5 wt % blend exhibited turbidity traces that were difficult to interpret with regard to crystallization kinetics (Figure B.3a). At first glance, sheared samples appeared to crystallize slower, reaching 80% transmittance multiple decades later than samples crystallizing quiescently. However, this lag is the result of the development of a local

minimum that resembles that of HDPE blends in Chapter 5 (Figure 5.5).

Apparent birefringence traces of all sheared samples exhibit increased values during shear as a consequence of flow birefringence (Figure B.3b). However, the immediate drop in  $I_{perp}/I$  following cessation of shear indicates that no anisotropic structures were formed.<sup>3, 26</sup>

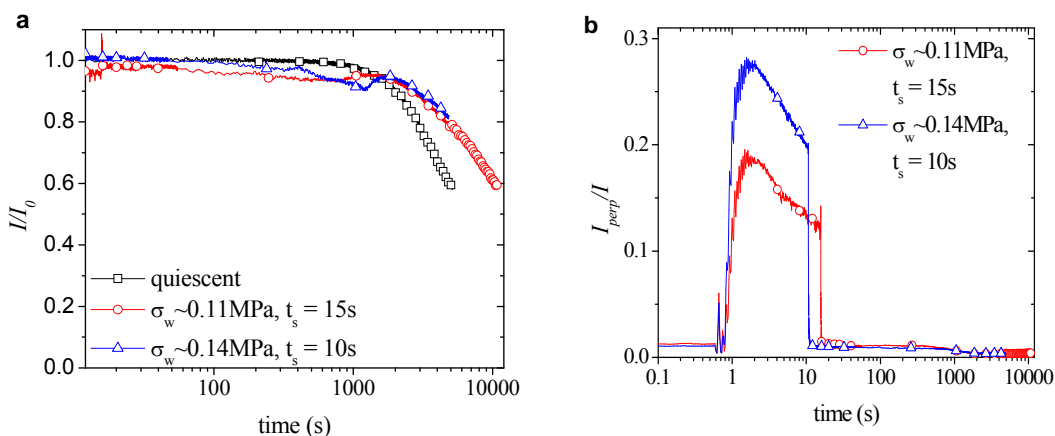


**Figure B.3 a)** Transmittance ( $I/I_0$ ) and **b)** apparent birefringence ( $I_{perp}/I$ ) for 5 wt % comb blend sheared at 98 °C.

## B.4 DISCUSSION

Comb blends did not exhibit the expected behavior in response to shear. For reference, the evolution of transmittance and apparent birefringence is provided in Figure B.4 for an isotactic polypropylene (iPP) sample. In response to shear, this sample exhibited the expected enhancement of crystallization kinetics (evidenced by the shorter time to reach 50% transmittance in Figure B.4a) and oriented crystal growth (evidenced by growth in birefringence after cessation of shear in Figure B.4b). For iPP, the monotonic trend in the transmittance allows us to relate increased turbidity of the sample to its crystallinity development, contrary to blends of the HPBD (above) and HDPE

(Chapter 5). In highly oriented samples, apparent birefringence exhibits sinusoidal behavior (see eq 5.3 in Chapter 5).<sup>19, 27</sup> A comparison between Figure B.3b and Figure B.4b quickly reveals a complete lack of oriented growth.

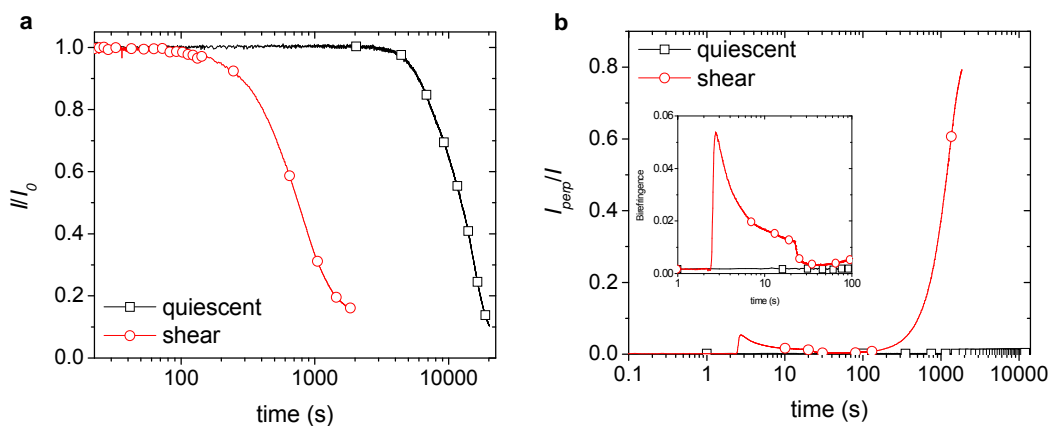


**Figure B.4 a)** Transmittance and **b)** apparent birefringence comparisons for sheared and quiescently crystallized iPP presented for comparison.

This surprising result is not a consequence of a lack of comb chain orientation in response to the flow field. The degree of orientation expected for comb chains can be inferred from the Wiessenberg number ( $Wi$ ),<sup>28-31</sup> which is a ratio of the relaxation time of the chains to the time scale for the shear process. The orientation of chains by flow is expected for  $Wi > 1$ . For the current shear process,

$$Wi = \dot{\gamma} \tau_{r,comb}, \quad (B.3)$$

where  $\tau_{r,comb}$  is the characteristic relaxation time of the comb chains. The shear rate,  $\dot{\gamma}$ , can be estimated from

$$\dot{\gamma} \sim \frac{\sigma_w}{\mu}, \quad (B.4)$$

where  $\mu$  is the viscosity of the blend. The viscosity is related to the relaxation modulus,  $G$ , as

$$\mu = \int_0^{\infty} G(t) dt \sim G_N^0 \tau_r . \quad (\text{B.5})$$

The approximation of  $\mu$  as the product of the plateau modulus,  $G_N^0$ , and terminal relaxation time,  $\tau_r$ , is valid for monodisperse, entangled, linear melts. Given that the current sample only meets the entangled criterion, we acknowledge that this is not a rigorous calculation but, rather, an order of magnitude estimate. Using  $G_N^0 \sim 1$  MPa for polyethylene,<sup>32</sup>  $\sigma_w \sim 0.1$  MPa, and the terminal relaxation time of the melt,  $\tau_r \approx 0.005$  s,<sup>33</sup> the shear rate for these experiments determined to be approximately  $20 \text{ s}^{-1}$ . The comb polymer has a terminal relaxation time of  $7.5 \text{ s}$ ,<sup>34</sup> resulting in  $Wi \sim 100$ . Hence, we expect the comb chains to be strongly oriented by flow.

The unusual transmittance curves (Figure B.3a) further support the deformation of chains from their equilibrium configurations during shear. When combs are above their overlap concentrations (i.e., 5 wt % blend), sample transmittance decreases to a minimum following the cessation of shear, recovers slightly, and resumes a monotonic decrease at a slower rate than in the quiescent case. This behavior is most pronounced at highest shear stress suggesting that it is a consequence of chain response to the flow field.

Since we expect the orientation of comb chains by the flow field, the lack of subsequent oriented growth must be the result of the inability of the system to effectively propagate oriented crystals from these chains. Given the strong effect of SCB content on quiescent crystallization (see Chapter 3 and references within), we anticipate that these chain defects are to blame for the lack of oriented growth.

## B.5 CONCLUSION

Application of a flow field to bimodal blends containing well-defined HPBD combs at concentrations above their overlap concentration did not result in typical flow-induced crystallization behavior. Although comb chains were oriented by the application of a shear pulse ( $Wi \gg 1$ ), subsequent oriented growth was not observed. This lack of oriented morphology can be accounted for by either (1) a lack of oriented nuclei formation from the oriented chains, or (2) if oriented nuclei did form, the inability of the melt to effectively propagate oriented growth from the nuclei. We hypothesize that either scenario can be a consequence of the relatively high short-chain branching content of both the base resin (EH50 having 23.2 SCB/1000 backbone C) and the slow-relaxing comb polymer (C4 having 24.4 SCB/1000 backbone C).

To further examine this theory, we propose FIC studies on the same high-SCB-content base resin (EH50) but blended with small amounts of a high- $M_w$  (i.e., slow-relaxing) high-density polyethylene (HDPE). The latter molecule is well-known to form oriented nuclei,<sup>35-38</sup> hence, the effect of SCB content on the propagation of an oriented morphology can be examined. These studies (described in Chapter 5) can provide further insight into the crystallization of industrially relevant linear-low density polyethylenes (LLDPE).

## B.6 ACKNOWLEDGEMENTS

This work would not have been possible without ExxonMobil Research and Engineering Company, particularly Dr. David Lohse, Dr. Cynthia Mitchell, Dr. Jung Hun Lee and the rest of the team, who provided materials, financial support, experimental

assistance, and fruitful discussions. Additionally, the model materials examined here were graciously provided by Prof. Nikos Hadjichristidis (University of Athens, Athens, Greece) and made available through collaboration with ExxonMobil. Experimental assistance was also provided by Dr. Lucia Fernandez Ballester. Additional funding was provided by the National Science Foundation (DMR-0505393 and GOALI-0523083). Manuscript preparation was assisted by Mary Louie (Caltech).

## B.7 REFERENCES

1. Liedauer, S.; Eder, G.; Janeschitz-Kriegl, H.; Jerschow, P.; Geymayer, W.; Ingolic, E., On the kinetics of shear-induced crystallization in polypropylene. *International Polymer Processing* **1993**, 8, (3), 236-244.
2. Bond, E. B.; Spruiell, J. E., Melt spinning of metallocene catalyzed polypropylenes. I. On-line measurements and their interpretation. *Journal of Applied Polymer Science* **2001**, 82, (13), 3223-3236.
3. Kumaraswamy, G.; Kornfield, J. A.; Yeh, F.; Hsiao, B. S., Shear-Enhanced Crystallization in Isotactic Polypropylene. 3. Evidence for a Kinetic Pathway to Nucleation. *Macromolecules* **2002**, 35, 1762-1769.
4. Haas, T. W.; Maxwell, B., Effects of Shear Stress on Crystallization of Linear Polyethylene and Polybutene-1. *Polymer Engineering and Science* **1969**, 9, (4), 225-&.
5. Andersen, P. G.; Carr, S. H., Crystal Nucleation in Sheared Polymer Melts. *Polymer Engineering and Science* **1978**, 18, (3), 215-221.
6. Kantz, M. R.; Stigale, F. H.; Newman, H. D., Skin-Core Morphology and Structure-Property Relationships in Injection-Molded Polypropylene. *Journal of Applied Polymer Science* **1972**, 16, (5), 1249-&.
7. McLeish, T. C. B., Hierarchical-relaxation in tube models of branched polymers. *Europhysics Letters* **1988**, 6, (6), 511-516.
8. Hadjichristidis, N.; Xenidou, M.; Iatrou, H.; Pitsikalis, M.; Poulos, Y.; Avgeropoulos, A.; Sioula, S.; Paraskeva, S.; Velis, G.; Lohse, D. J.; Schulz, D. N.; Fetters, L. J.; Wright, P. J.; Mendelson, R. A.; Garcia-Franco, C. A.; Sun, T.; Ruff, C. J., Well-

- defined, model long chain branched polyethylene. 1. Synthesis and characterization. *Macromolecules* **2000**, 33, (7), 2424-2436.
9. Bender, J. T.; Knauss, D. M., Synthesis of Low Polydispersity Polybutadiene and Polyethylene Stars by Convergent Living Anionic Polymerization. *Journal of Polymer Science: Part A: Polymer Chemistry* **2006**, 44, 828-836.
10. Driva, P.; Iatrou, H.; Lohse, D. J.; Hadjichristidis, N., Anionic Homo-and Copolymerization of Double-Tailed Macromonomers: A Route to Novel Macromolecular Architectures. *Journal of Polymer Science: Part A: Polymer Chemistry* **2005**, 43, 4070-4078.
11. Koutalas, G.; Iatrou, H.; Lohse, D. J.; Hadjichristidis, N., Well-Defined Comb, Star-Comb, and Comb-on-Comb Polybutadienes by Anionic Polymerization and the Macromonomer Strategy. *Macromolecules* **2005**, 38, 4996-5001.
12. Vazaios, A.; Lohse, D. J.; Hadjichristidis, N., Linear and Star Block Copolymers of Styrenic Macromonomers by Anionis Polymerization. *Macromolecules* **2005**, 38, 5468-5474.
13. Heeley, E. L.; Fernyhough, C. M.; Graham, R. S.; Olmsted, P. D.; Inkson, N. J.; Embery, J.; Groves, D. J.; McLeish, T. C. B.; Morgovan, A. C.; Meneau, F.; Bras, W.; Ryan, A. J., Shear-induced crystallization in blends of model linear and long-chain branched hydrogenated polybutadienes. *Macromolecules* **2006**, 39, 5058-5071.
14. Kumaraswamy, G., Crystallization of Polymers from Stressed Melts. *Journal of Macromolecular Science, Part C: Polymer Reviews* **2005**, 45, 375-397.

15. Seki, M.; Thurman, D. W.; Oberhauser, J. P.; Kornfield, J. A., Shear-mediated crystallization of isotactic polypropylene: The role of long chain -- long chain overlap. *Macromolecules* **2002**, 35, 2583-2594.
16. Hsiao, B. S.; Yang, L.; Somani, R. H.; Avila-Orta, C. A.; Zhu, L., Unexpected Shish-Kebab Structure in a Sheared Polyethylene Melt. *Physical Review Letters* **2005**, 94, (11).
17. Yang, L.; Somani, R. H.; Sics, I.; Hsiao, B. S.; Kolb, R.; Lohse, D., The role of high molecular weight chains in flow-induced crystallization precursor structures. *Journal of Physics: Condensed Matter* **2006**, 18, S2421-S2436.
18. Zuo, F.; Keum, J. K.; Yang, L.; Somani, R. H.; Hsiao, B. S., Thermal Stability of Shear-Induced Shish-Kebab Precursor Structure from High Molecular Weight Polyethylene Chains. *Macromolecules* **2006**, 39, 2209-2218.
19. Fernandez-Ballester, L.; Gough, T.; Meneau, F.; Bras, W.; Ania, F.; Balta-Calleja, F. J.; Kornfield, J. A., Simultaneous birefringence, small- and wide-angle X-ray scattering to detect precursors and characterize morphology development during flow-induced crystallization of polymers. *Journal of Synchrotron Radiation* **2008**, 15, (2), 185-190.
20. Rachapudy, H.; Smith, G. G.; Raju, V. R.; Graessley, W. W., Properties of Amorphous and Crystallizable Hydrocarbon Polymers .3. Studies of the Hydrogenation of Polybutadiene. *Journal of Polymer Science Part B-Polymer Physics* **1979**, 17, (7), 1211-1222.
21. Krigas, T. M.; Carella, J. M.; Struglinski, M. J.; Crist, B.; Graessley, W. W.; Schilling, F. C., Model Copolymers of Ethylene with Butene-1 Made by

- Hydrogenation of Polybutadiene - Chemical Composition and Selected Physical Properties. *Journal of Polymer Science: Part B: Polymer Physics* **1985**, 23, (3), 509-520.
22. Kapnistos, M.; Vlassopoulos, D.; Roovers, J.; Leal, L. G., Linear Rheology of Architecturally Complex Macromolecules: Comb Polymers with Linear Backbones. *Macromolecules* **2005**, 38, 7852-7862.
23. deGennes, P.-G., *Scaling Concepts in Polymer Physics*. Cornell University Press: Ithica, NY, 1979.
24. Takahashi, Y.; Isono, Y.; Noda, I.; Nagasawa, M., Zero-Shear Viscosity of Linear Polymer Solutions over a Wide Range of Concentration. *Macromolecules* **1985**, 18, (5), 1002-1008.
25. Crist, B.; Tanzer, J. D.; Graessley, W. W., Small-Angle Neutron-Scattering of a Model Crystallizable Polymer - Crystallization and Size-Mismatch Effects. *Journal of Polymer Science Part B - Polymer Physics* **1987**, 25, (3), 545-556.
26. Kumaraswamy, G.; Verma, R. K.; Kornfield, J. A., Novel flow apparatus for investigating shear-enhanced crystallization and structure development in semicrystalline polymers. *Review of Scientific Instruments* **1999**, 70, (4), 2097-2104.
27. Kumaraswamy, G.; Issaian, A. M.; Kornfield, J. A., Shear-Enhanced Crystallization in Isotactic Polypropylene. 1. Correspondence between in Situ Rheo-Optics and ex Situ Structure Determination. *Macromolecules* **1999**, 32, (22), 7537-7547.
28. Beek, M. H. E. V. d.; Peters, G. W. M.; Meijer, H. E. H., Classifying the Combined Influence of Shear Rate, Temperature, and Pressure on Crystalline Morphology and Specific Volume of Isotactic (Poly)propylene. *Macromolecules* **2006**, 39, 9278-9284.

29. Acierno, S.; Palomba, B.; Winter, H. H.; Grizzuti, N., Effect of molecular weight on the flow-induced crystallization of isotactic poly(1-butene). *Rheologica Acta* **2003**, 42, (3), 243-250.
30. Elmoumni, A.; Winter, H. H.; Waddon, A. J.; Fruitwala, H., Correlation of material and processing time scales with structure development in isotactic polypropylene crystallization. *Macromolecules* **2003**, 36, (17), 6453-6461.
31. Bustos, F.; Cassagnau, P.; Fulchiron, R., Effect of molecular architecture on quiescent and shear-induced crystallization of polyethylene. *Journal of Polymer Science Part B - Polymer Physics* **2006**, 44, (11), 1597-1607.
32. Rubinstein, M.; Colby, R. H., *Polymer Physics*. Oxford University Press: New York, 2003.
33. Rheology studies were graciously conducted by Dr. Juhn Hun Lee at ExxonMobil (Clinton, NJ).
34. Rheology studies were graciously conducted by Dr. Juhn Hun Lee at ExxonMobil (Clinton, NJ).
35. Langouche, F., Orientation development during shear flow-induced crystallization of i-PP. *Macromolecules* **2006**, 39, 2568-2573.
36. Pople, J. A.; Mitchell, G. R.; Sutton, S. J.; Vaughan, A. S.; Chai, C. K., The development of organized structures in polyethylene crystallized from a sheared melt, analyzed by WAXS and TEM. *Polymer* **1999**, 40, (10), 2769-2777.
37. Liang, S.; Wang, K.; Tang, C. Y.; Zhang, Q.; Du, R. N.; Fua, Q., Unexpected molecular weight dependence of shish-kebab structure in the oriented linear low

- density polyethylene/high density polyethylene blends. *Journal of Chemical Physics* **2008**, 128, (17), 9.
38. Somani, R. H.; Yang, L.; Zhu, L.; Hsiao, B. S., Flow-induced shish-kebab precursor structures in entangled polymer melts  
*Polymer* **2005**, 46, 8587-8623.